Journal of Pharmaceutical and Biomedical Analysis 158 (2018) 461–470

Contents lists available at ScienceDirect

Journal of Pharmaceutical and Biomedical Analysis

journal homepage: www.elsevier.com/locate/jpba

Chemometrics-assisted study of the interconversion between the crystalline forms of nimodipine

Natalia L. Calvo[a,b], Naira M. Balzaretti[c], Marina Antonio[b], Teodoro S. Kaufman[a,b,*], Rubén M. Maggio[a,b,*]

[a] Institute of Chemistry of Rosario (IQUIR, CONICET-UNR), Suipacha 531, Rosario S2002LRK, Argentina
[b] Pharmaceutical Analysis, Department of Organic Chemistry, School of Pharmaceutical and Biochemical Sciences, National University of Rosario, Suipacha 531, Rosario S2002LRK, Argentina
[c] Institute of Physics, Universidade Federal do Rio Grande do Sul, Av. Bento Gonçalves 9500, Caixa Postal 15051, Barrio Agronomia, Porto Alegre RSCEP91501-970, Brazil

ARTICLE INFO

Article history:
Received 20 February 2018
Received in revised form 11 June 2018
Accepted 12 June 2018
Available online 18 June 2018

Keywords:
Nimodipine
ATR-FTIR
Multivariate curve resolution with alternating least squares
Chemometrics
Polymorphic interconversion

ABSTRACT

Nimodipine (NIM) is a calcium channel-blocking agent, which in the solid state exhibits two crystalline modifications, Mode I and Mode II. The first one is a racemic mixture, while the second is a conglomerate. Because the drug has poor aqueous solubility and Mode I is twice as soluble as Mode II, the former is widely preferred for the development of pharmaceutical forms. In order to study the effect of thermal stimuli on the behavior of NIM, an analytical method was developed coupling ATR-FTIR spectroscopy to Multivariate Curve Resolution with Alternating Least Squares (MCR-ALS). The method allowed to monitor the transformations of each polymorph, their respective mixtures and commercial samples, during the thermal treatment.

It was observed that Mode II experienced changes during the experiments and the chemometric technique provided the abundance profile and the pure spectra of the different species involved. In this way, it was established that Mode II has two transitions, at 116.8 °C and 131.9 °C, which reflect that Mode II is first transformed into Mode I, which then melts. The liquid phase solidifies to give an amorphous (AM) vitreous solid, which does not revert to the crystalline state. The analysis of a commercial sample of NIM exhibited the similar transformations than Mode II; however, a pronounced decrease was noted in the first transition temperature (95 °C), whereas the second remained essentially unchanged (131.6 °C). This could be a result of the presence of mixtures of Mode I and Mode II (0.32:0.68) in the bulk solid, as confirmed by the analysis of a physical mixture of crystals of Modes I and II.

Therefore, it was concluded that the developed ATR-FTIR/MCR-ALS method is suitable for the detailed analysis of the crystalline forms of NIM in bulk drug and enables de study of their possible thermally promoted interconversions.

1. Introduction

The quality of pharmaceutical products is currently controlled based a scientific understanding of their manufacturing processes, and the most thorough knowledge of their quality attributes. Most active pharmaceutical ingredients (API) are solids and they are prescribed as solid dosage forms. Many of them can adopt various crystalline configurations in their solid-state form, which differ in their spatial lattice and/or in their molecular conformations.

This phenomenon, termed polymorphism, may have impact on the properties of these chemical entities while they remain in solid state. The API processability during manufacture, for instance, depends on density, particle shape and size, and its resulting flowability. In addition, different polymorphs may have distinct solubility and dissolution rate, stability, therapeutic efficacy, toxicity and bioavailability, among other critical features [1]. Polymorphs may also undergo phase transformations during processing and storage, affecting the product quality [2].

Nimodipine (NIM) is 3-isopropyl 5-(2-methoxyethyl)-2,6-dimethyl-4-(3-nitrophenyl)-1,4-dihydropyridine-3,5-dicarboxylate (Fig. 1). The drug has one stereogenic center,

* Corresponding authors at: Institute of Chemistry of Rosario (IQUIR, CONICET-UNR), Suipacha 531, Rosario S2002LRK, Argentina.
E-mail addresses: kaufman@iquir-conicet.gov.ar (T.S. Kaufman), maggio@iquir-conicet.gov.ar (R.M. Maggio).

https://doi.org/10.1016/j.jpba.2018.06.019
0731-7085/

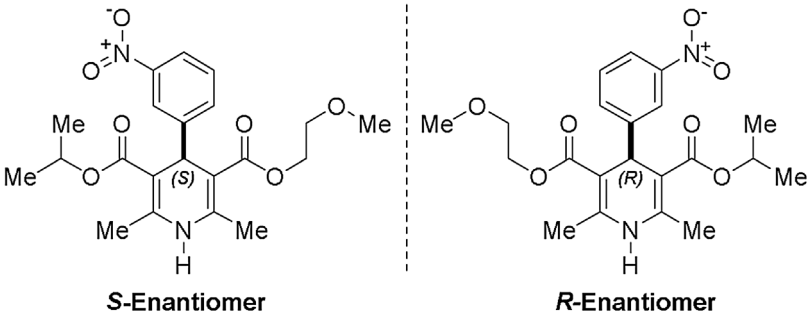

Fig. 1. Chemical structures of the enantiomers of NIM, as mirror images.

which enables the existence of stable and chromatographically separable *R* and *S* enantiomers, as distinct chemical entities [3]; however, this API is currently marketed as the racemate.

NIM is a dihydropyridine-type calcium channel blocking agent, originally developed as a hypertensive compound, but currently prescribed for improving the neurological outcome of patients with subarachnoid hemorrhage, by reducing the incidence and severity of their ischemic deficits due to its ability to cross the blood-brain barrier and dilate the cerebral arterioles [4]. The drug is marketed worldwide in the forms of tablets, oral solutions and intravenous infusions [1,5].

NIM presents two solid state forms, known as Modification I (Mode I) and Modification II (Mode II) [6]. Mode I refers to a racemic compound containing an equimolar mixture of the *R*- and *S*- enantiomers of the drug in the same unit cell. On the other hand, Mode II is a conglomerate, where each enantiomer crystallizes in a different unit cell, and both solid phases form an equimolar mixture, as shown in the seminal work of Grunenberg et al. [7].

This API belongs to the Class 2 of the Biopharmaceutical Classification System (BCS), because it is practically insoluble in water but has high permeability to biological membranes [5,8]. In agreement with this classification, the drug exhibits low bioavailability after oral administration [8], and the dissolution rate in gastrointestinal fluids is the limiting stage in the absorption of NIM.

The solubility of Mode I in water is at least twice that of Mode II at 25 °C and 37 °C (0.86 and 0.44 mg L^{-1}, respectively) [7]. Hence, although Mode I is more sensitive to photochemical decomposition [9], it is the polymorph required for the manufacture of pharmaceutical dosage forms. However, Mode II is often present in different quantities as a crystalline impurity, usually diminishing, but sometimes compromising the quality of this active pharmaceutical ingredient [10].

Liu et al. reported that NIM tablets administered to healthy Chinese men exhibited great pharmacokinetics variability [11]. Subsequent studies revealed that the different polymorphs contained in the samples were responsible for such results. In addition, a recent report on the recrystallization of NIM in a generic drug product motivated the recall of commercial lots of the pharmaceutical product from the market [12]. Therefore, the most complete understanding of the polymorphic composition of NIM solid state products is deemed extremely important [13].

Different strategies have been implemented to improve the dissolution of NIM, including complexation with cyclodextrins [14], micronization [15], solid dispersions in polyethylene glycol (PEG) 2000–8000 [8,16,17] and poly(vinylpyrrolidone) [18,19], and the use of nanocrystals [20], among others.

In addition, special aqueous (acetate buffer pH 4.5 with 0.05% SDS) [21] and hydro-alcoholic [1:1 (*v*/*v*) EtOH:H_2O] [22] dissolution media have been devised to differentiate between both forms according to their dissolution properties.

The stability of the polymorphs of NIM was studied through the evaluation of the thermodynamic transition temperature of agitated suspensions of the drug containing both modifications in different solvents and at different temperatures [7]. Analysis of the residues after 8–96 h revealed the presence of Mode II at temperatures below 80 °C, while at 95 °C andabove only Mode I was found.

It has also been noticed that no polymorphic transformation takes place in the solvent-free drug, when it is stored for one year at −40 °C to +50 °C at a pressure of 9 kbar. However, the presence of even traces of solvents, like isopropanol or ethanol, is enough to accelerate the transformation of the thermodynamically metastable Mode I into Mode II, which is stable at room temperature [7].

Furthermore, polymorphic transformations of NIM were recorded during high-cut shear granulation [6], in the preparation of micro- and nanocrystals by the microprecipitation technique [23] and in PEG-based hot-melt extrudates [24].

The non-aqueous volumetric official assays of NIM in the American, European and British Pharmacopeias do not provide any information about the content or identity of the polymorphic forms of NIM in the analytical sample. Awareness of the problem resulted in the recent development of quantitative methods for the determination of the polymorphs of NIM, using differential scanning calorimetry [25,26], solid-state NMR (ssNMR), X-ray powder diffraction (XRPD) [27] and vibrational spectroscopies (NIR, FTIR, Raman) [12], in bulk drug and in pharmaceutical formulations [24].

Some of these methods included associations to chemometrics techniques for better performance, because chemometrics has evolved into a particularly well-suited set of vibrational spectroscopies for the study of the solid state of pharmaceutical ingredients [28,29].

Therefore, reported herein is a new methodology suitable for monitoring the thermal transformations between the polymorphic forms of nimodipine in the bulk drug. This approach is based on coupling attenuated total reflectance infrared spectroscopy (ATR-FTIR) to multivariate curve resolution with alternating least squares (MCR-ALS) as a chemometrics tool. The application of the methodology to a commercial sample, which allowed to estimate its polymorph richness without any additional calculation, is also presented.

2. Materials and methods

2.1. Instrumentation and software

The pure solid-state forms were sieved separately with an RR1920 Zonitest Vibration system (Rey & Ronzoni, Buenos Aires, Argentina), fitted with ASTM-certified stainless-steel sieves, to a particle size between 50 and 100 mesh.

The crystallinity of the samples was examined by X-ray diffraction analysis (XRD), performed in random and oriented powders, using a Siemens D-500 powder diffractometer, equipped with a Cu-Kα source. The wavelength was 1.5406 Å (40 kV, 40 mA) and Soller slots in the incident beam, a 1° divergence slot, a 0.15 mm input slot and a graphite monochromator in the secondary beam were used. The data were collected over a 2θ angular range of 2–60°, with a step size of 0.05° and a counting time of 1 s per step for all samples.

The Raman spectra were acquired using a Micro-Raman instrument, with a 10 mW laser and an excitation wavelength of 632.8 nm. The laser micro-beam had approximately 2 μm in diameter and, during the measurements, the sample was randomly moving horizontally to avoid local heating and sample damage. The scattered radiation was collected during an acquisition time of 5 s in the region between 500 and 4000 cm^{-1}.

A Zeiss EVO 50 scanning electron microscope (SEM) was employed to observe the morphology of the samples. Before the analysis, the samples were coated with a thin gold film (15–20 nm thick) using a BalTec SCD 050 Sputter coater at a metallization time of 80 s, a current of 40 mA and at a vacuum of 5×10^{-2} mBar. The samples were placed on metallic stubs with double-sided conductive carbon tape coated in gold.

The estimation of the particle size was performed by analysis of the SEM images with the Image-pro Plus software v. 6.0, calculating Feret's diameter, as the distance between the two furthest points of the shape measured in a given direction [30]. A set of 200 crystals was taken for each determination.

The DSC analysis was performed in a Shimadzu 60 differential scanning calorimeter, operating under a dry nitrogen atmosphere at a constant flow of 30 mL/min. The thermograms were recorded between 40 °C and 140 °C, with 2–3 mg of accurately weighed samples placed in a closed aluminum pan with a small perforation to allow pressure equilibrium, avoiding expansion of developed gases or residual solvents. The heating rate was 2 °C min^{-1} and an empty container was used as a reference.

The mid infrared spectra were acquired in a Shimadzu Prestige 21 FTIR spectrophotometer coupled to a GladiATR (Pike Technology) ATR accessory, with temperature control. Twenty scans were acquired per sample, at a resolution of 4 cm^{-1}. The particle size, amount of sample and pressure exerted on the sample were standardized. After analyzing each sample, the powder was removed and the equipment was carefully cleaned with a 50:50 (*v/v*) mixture of water:isopropanol. Background spectra were obtained against air using a clean and dry ATR accessory.

The computing routines involving spectral data manipulation and the MCR-ALS method were processed in Matlab R2008 (Mathworks, Natick, USA). Statistical data analyses and graphic plots were developed with Origin 8.0 (OriginLab Co., Northampton, USA).

2.2. Active pharmaceutical ingredients and chemicals

Pharmaceutical grade NIM (USP XXIV), containing a mixture of polymorphs, was acquired from Droguería Saporiti (Argentina).

The polymorphs used in this work were prepared in our laboratory through different techniques (see Section 2.3).

All solvent employed in the following procedures were in analytical grade.

2.3. Preparation of the polymorphs of NIM

NIM Mode I was obtained by stirring under reflux (97 °C) for 2 days a saturated solution of NIM in propanol in the presence of a solid sediment. Then, the system was filtered while heated and dried in a vacuum oven at 95 °C and −50 mmHg for 5 days.

NIM Mode II was obtained by stirring for 3 days at room temperature a saturated solution of NIM in 2-propanol, to which an excess of NIM was added. Then, the system was centrifuged and the solid residue was placed in a vacuum oven at 50 °C and −50 mmHg for 4 days [7].

Both pure solid forms were stored in a desiccator, in hermetic caramel glass recipient and protected from light in order to avoid photolysis.

Table 1
Physical properties of NIM Mode I and Mode II.

	Mode I	Mode II
Crystallization type	Racemic	Conglomerate
Color	Yellow	Off-white
Stability range	>90 °C-melting point	0-90
Melting point (°C)	125.0	115.5
Heat of fusion (Kj mol^{-1})	38.4	46.7

2.4. Study of the polymorphic interconversion. Thermal ATR-FTIR sample analysis

Each sample (~20 mg) was placed on the ATR accessory window and properly pressed. The sample was subjected to temperatures between 30–148 °C in the heating plate of the ATR, while twenty-six spectral readings were acquired for each sample at pre-established temperatures, every 10° between 30–100 °C (8 spectra), every 2 °C between 105–133 °C (15 spectra) and every 5 °C between 138–148 °C (3 spectra).

2.4.1. Preparation of the samples

The samples of NIM under analysis were Mode I, Mode II, mixtures of Mode I/Mode II and commercial bulk drug.

For all samples, the particle size was homogenized by sieving (50–100 mesh); the mass of the components was accurately weighed, and their composition homogeneity was reached by mixing in a Z-mixer at 50 rpm during 30 min.

3. Results and discussion

3.1. Characterization of the NIM polymorphs

3.1.1. Visual examination

To the naked eye, Mode I and Mode II presented visible color differences. Mode I was yellow while Mode II was almost white (Table 1). This is due to differences in the position of the nitro moiety with respect to the phenyl ring in the crystals. The angle between the planes of the NO_2 group and the phenyl ring is 1° in Mode I and 9° in Mode II. The almost coplanar arrangement in Mode I favors conjugation between both moieties, producing a bathochromic spectral shift [7]. In order to fully ensure their identity and purity, both forms were exhaustively characterized, employing different techniques.

3.1.2. Scanning electron microscopy (SEM)

The morphological differences in shape and size of the crystals were visualized by scanning electron microscopy. The Mode I micrographs were examined at 250× (Fig. 2A), whereas the Mode II microcrystals were better observed at 2500× and 5000× (Fig. 2C and D, respectively). No special geometrical arrays can be observed in the micrographs of the crystals of both modifications. However, the smoothness of the surface of the crystals of Mode II is clearly observed at the magnifications of 5000×. On the other hand, the particle size analysis (Fig. 2B) evidenced a more homogeneous distribution of semi-spherical particles in the sample of Mode II, while for Mode I all kinds of shapes are interspersed.

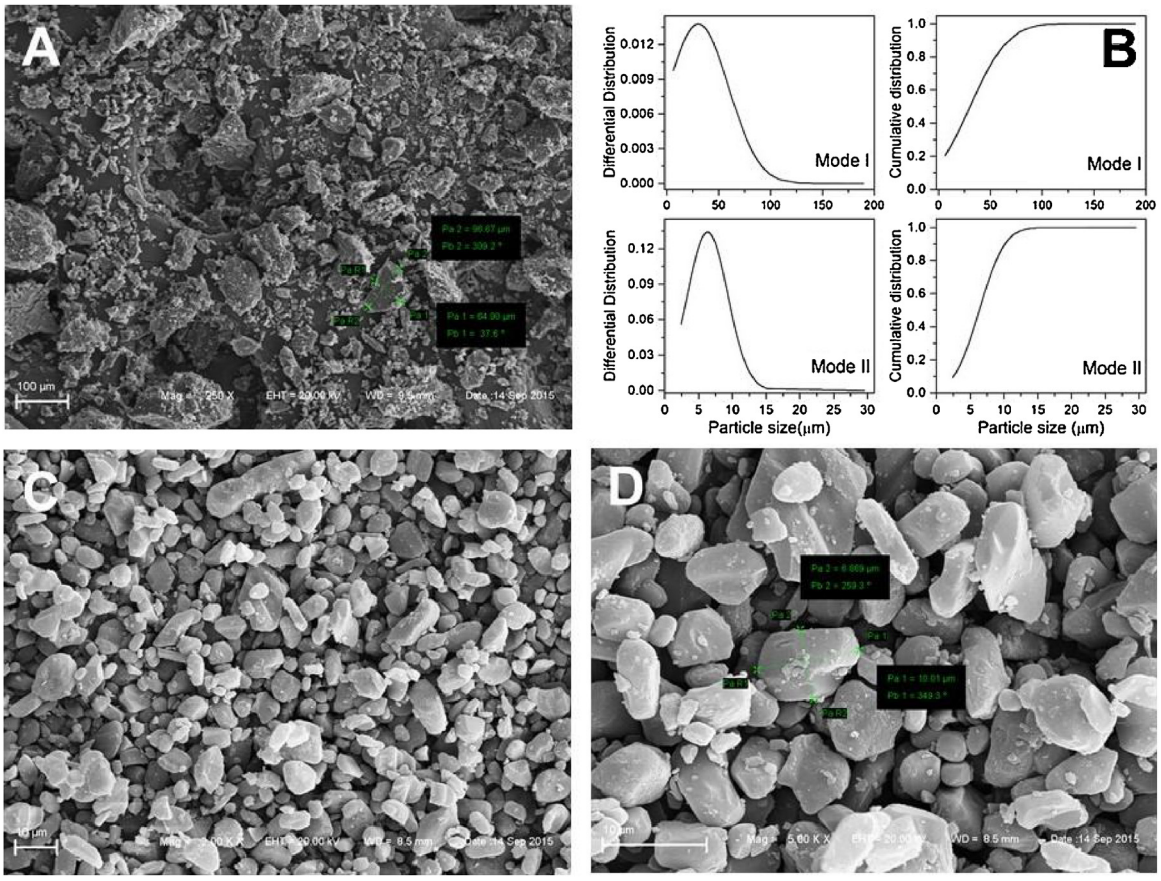

Fig. 2. SEM micrographs and particle size distribution of NIM crystals. A) Mode I at 250×. B) Particle size distribution in the crystal forms. C) Mode II at 2000× and D) Mode II at 5000×.

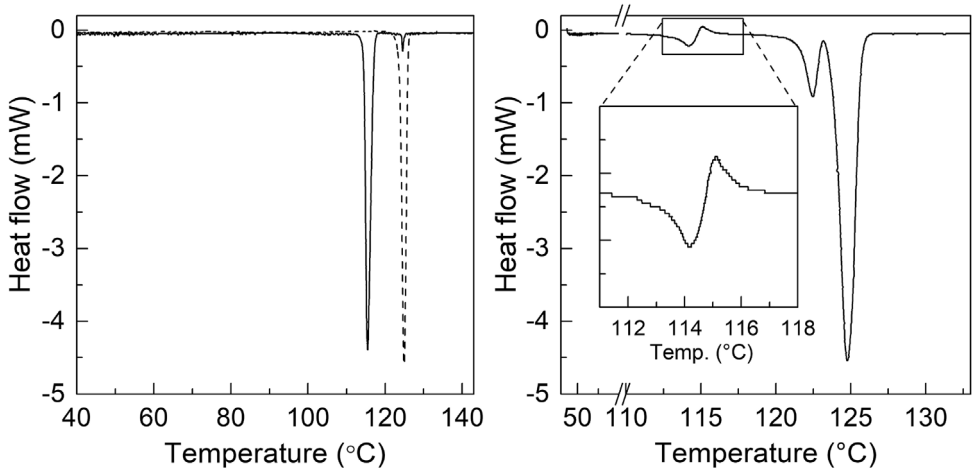

Fig. 3. A) DSC thermograms for Mode I (—) and Mode II (––) of NIM. B) DSC thermogram of the commercial bulk drug.

3.1.3. Differential scanning calorimetry (DSC)

The DSC thermograms of NIM Mode I and II (Fig. 3A) showed endothermic transitions at 124.98 °C, and 115.5 °C, respectively (Table 1). It was also observed that the heat of fusion of Mode (46.7 kJ mol^{-1}) was significantly higher than that of Mode I (38.4 kJ mol^{-1}).

Taking into account that the thermogram belonging to Mode II presented a small peak at 124.6 °C that could be assigned to Mode I, the integration of the areas was used according to the literature, to determine the abundance of Mode I, which resulted in 1.37% [25]. The so estimated purity of Mode II was evaluated as satisfactory for the development of the proposed study. It is worth to be mentioned that systems containing Form II (conglomerate) and Form I (racemic compound) of nimodipine give rise to eutectic mixtures [7], turning unreliable the quantitation of the polymorphs and their ratio by DSC.

3.1.4. Raman spectroscopy

Although the NIM modifications exhibited similar Raman spectra, the relative intensities of the peaks were not alike (Fig. 4A and B).

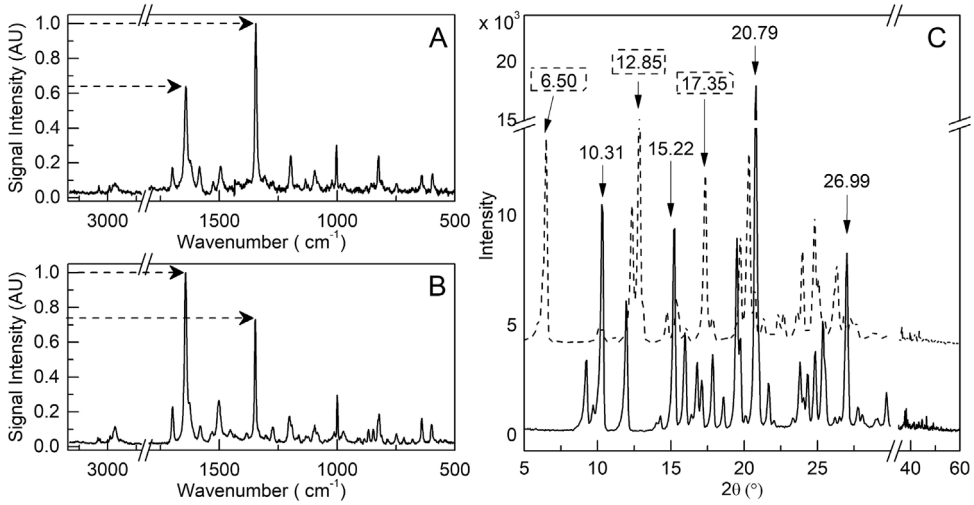

Fig. 4. A) Raman spectrum of NIM Mode I. B) Raman spectrum of NIM Mode II. C) X-ray diffraction patterns of NIM Mode I (—) and NIM Mode II (––).

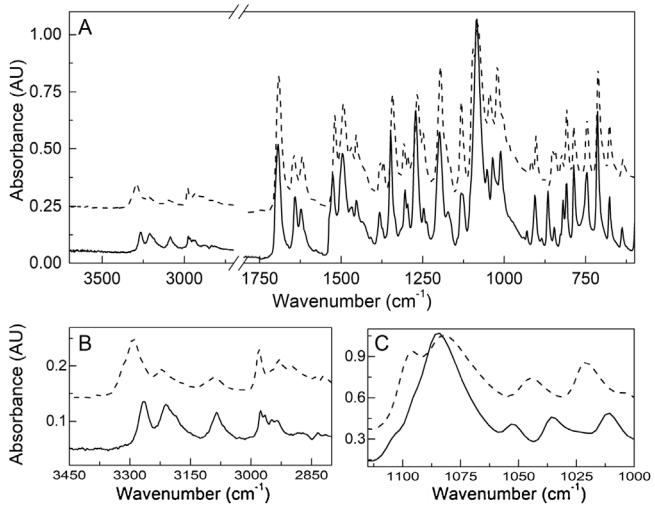

Fig. 5. ATR-FTIR spectra of NIM Mode I (—) and NIM Mode II (––). A) Full spectra. B) Spectra in the 3450–2800 cm^{-1} range. C) Spectra in the 1115–1000 cm^{-1} interval.

Intensity inversions were observed in the signal related to the C=C stretching of the dihydropyridine ring, located at 1643 cm^{-1}, which proved to be greater for Mode II, whereas the fluorescence of the symmetrical stretching of the NO_2 group (at 1347 cm^{-1}) was more intense for Mode I and of higher intensity than that observed in 1643 cm^{-1}. As a result, the ratio of intensities I_{1347}/I_{1643} is > 1 for Mode I (I_{1347}/I_{1643} = 1.35), being < 1 for Mode II (I_{1347}/I_{1643} = 0.54) [8].

3.1.5. X-ray powder diffraction (XRD)

The XRD analysis of the powder showed very different diffractograms for both forms (Fig. 4C), especially at low angles (2θ), which allowed easy discrimination between the polymorphs. The main diffractions for Mode I was observed at 2θ values of 6.50°, 12.85° and 17,35°, while Mode II exhibited typical signals in 2θ values of 10.31°, 15.22°, 20.78° and 26.99°, in full agreement with the literature [6,31].

3.1.6. ATR-FTIR spectroscopy

The mid infrared spectra (FTIR) of the polymorphs were acquired at 30 °C by the ATR technique and are displayed in Fig. 5.

A summary of the characteristic bands for each Mode and their assignments are presented in Table 2. The main bands in the infrared spectra of NIM can be assigned to its secondary amine (—NH), the carbonyl ester (–CO_2–) and ether (—C—O—) groups, the nitro moiety (—NO_2), the aromatic —C=C— stretches and the aliphatic structure –CH [12,32].

Table 2
Characteristic bands of Mode I and Mode II of NIM in their FTIR spectra.

Mode I	Assignment	Mode II
3292	N—H	3265
3094	C—H	3085
2931	C—H aliphatic	2935
1691	C=O ester	1693
1645	C=C dihydropyridine ring	1642
1620	C=C aromatic	1624
1520	N=O asymmetric	1526
1380	C—CH_3	1382
1342	N=O symmetric	1348
1132	C—O ether	1130
1044	Fingerprint	–

NIM presented the bands related to the asymmetric and symmetric stretching of the —NO_2 group at 1520 cm^{-1} and 1342 cm^{-1} for Mode I and at 1526 and 1348 cm^{-1} for Mode II [33,34]. Similarly, the stretching signal of the secondary N—H amino group was observed at 3292 cm^{-1} and 3265 cm^{-1} for Mode I and Mode II, respectively [31,35,36].

In the case the aromatic C=C and dihydropyridine C=C stretching bands, they were found at 1620 cm^{-1} and 1624 cm^{-1} for Mode I, while Mode II presented them at 1645 cm^{-1} and 1642 cm^{-1}, respectively [33,37]. Finally, examination of the fingerprint region revealed a peak at 1044 cm^{-1} only for Mode I, whereas Mode II exhibited a valley.

3.2. MCR-ALS analysis of thermal ATR-FTIR spectra. Method development

In order to unveil the constituents involved during the transformation of Mode I and II, the processes were monitored by FTIR using a heated plate ATR accessory, and further analyzed by MCR-ALS.

Hence, Mode I and Mode II were sequentially submitted to the thermal treatment in the temperature range between 30–148 °C, which includes the melting point of the solids, and the spectra were acquired at pre-specified temperatures (Section 2.1).

For further processing and analysis, the set of spectra collected during the heating process of each sample was arranged matrix-wise (temperature × wave number). The ordered data for each of

Table 3
Cumulative and explained variance of different PC models built from the set of ATR-FTIR spectra of NIM Mode I (A) and NIM Mode II (B), subjected to thermal treatment.

	Mode I		Mode II	
PC N°	Cumulative variance (%)	Explained variance (%)	Cumulative variance (%)	Explained variance (%)
1	89.03	89.03	69.61	69.61
2	**97.59**	**8.56**	94.36	24.45
3	99.06	1.47	**98.35**	**3.99**
4	99.46	0.40	99.08	0.73
5	99.63	0.17	99.45	0.37
6	99.72	0.09	99.66	0.21

Numbers in bold mean that these values are the most relevant and were used to make decisions.

the experiments were subsequently processed by Principal Component Analysis (PCA) in order to determine their chemical rank, *i.e.*, the number of different species responsible for the signal changes observed during the heating process (Table 3).

Then, the Multivariate Curve Resolution algorithm (MCR-ALS) was put in place to obtain the concentration profiles of the different species throughout the process, along with the infrared spectra of the corresponding "pure" species involved [38]. In order to confer physical sense to the results, restrictions such as non-negativity in the concentrations and spectral intensities were applied to the MCR-ALS system. The closure restriction was also added to the concentration values, in order to keep the sum of the relative abundances of the analytes invariable. The latter restriction was applied after assuming that no decomposition takes place during the process being studied and that, therefore, there is no change in the total number of moles of NIM along the whole operation.

The so obtained "pure" spectra were used to establish the identity of the species involved in the process. Additionally, the spectra coupled to their concentration profiles along the time revealed the nature of the resulting transformations and the transition temperatures.

In the first instance, Mode I was submitted to the thermal treatment and the PCA analysis of the corresponding FTIR data matrix revealed the presence of two components during heating (Table 3). By using the MCR-ALS algorithm on the full spectra initializing the system with two components (the starting Mode I and the final AM species), the species concentration profile shown in Fig. 6A revealed a transition temperature of 129.2 °C.

In order to assign the corresponding identities to the "pure" spectra obtained through the MCR-ALS calculations, these were statistically compared against the reference spectra of the solid forms Mode I, Mode II and that of the AM species. Pearson correlation coefficient was calculated and a cut-off value was arbitrarily set at $r = 0.950$ for the similarity tests.

Comparison of the first species given by MCR-ALS (S1) with the reference spectrum of Mode I, furnished a Pearson correlation coefficient (r) of 0.9943 when the full spectral region was employed for calculations (Table 4). Not significant values were obtained for the remaining species.

These results unequivocally suggested the identity of S1 was compatible with NIM Mode I. This hypothesis was further confirmed by analysis of the fingerprint (1650–600 cm^{-1}) and C–H/N—H stretching (3600–2500 cm^{-1}) regions, by separate.

On the other hand, the same statistical analysis was performed for S2, the second species provided by the MCR-ALS algorithm. This exhibited a coefficient $r = 0.9996$, when the comparison was carried out with the reference spectrum of the AM species and non-significant values were observed with the other suspected species ($r = 0.8943$ for Mode I and $r = 0.8420$ for Mode II). Thus, it was concluded that Mode I presented a single transformation at 129.2 °C,

Table 4
Pearson's correlation coefficients (r) of the pure spectra provided by MCR-ALS for Mode I and the reference spectra of the solid forms of NIM, in different spectral regions[a].

Source of the spectrum		Values of r in the given spectral region		
MCR	Solid form	Full spectrum (4000–600 cm^{-1})	Fingerprint (1650–600 cm^{-1})	C—H/N—H stretchings (3600–2500 cm^{-1})
Species 1	**Mode I**	**0.9943**	**0.9886**	**0.9666**
(S1)	Mode II	0.8987	0.8368	0.6150
	AM	0.9027	0.7474	0.6089
Species 2	Mode I	0.8943	0.7476	0.4855
(S2)	Mode II	0.8420	0.7496	0.2020
	AM	**0.9996**	**0.9991**	**0.9983**
Number of sensors (n)		1764	546	779

Numbers in bold mean that these values are the most relevant and were used to make decisions.
[a] The cut-off value for the similarity test at this stage was arbitrarily set at $r = 0.950$.

Table 5
Pearson's correlation coefficients (r) of the pure spectra provided by MCR-ALS for Mode II and the reference spectra of the solid forms of NIM, in different spectral regions[a].

Source of the spectrum		Values of r in the given spectral region		
MCR	Solid form	Full spectrum (4000–600 cm^{-1})	Fingerprint (1650–600 cm^{-1})	C—H/N—H stretchings (3600–2500 cm^{-1})
Species 1	Mode I	0.9375	0.8879	0.7270
(S1)	**Mode II**	**0.9936**	**0.9917**	**0.9776**
	AM	0.8683	0.7661	0.2594
Species 2	**Mode I**	**0.9832**	**0.9625**	**0.9501**
(S2)	Mode II	0.8844	0.8163	0.6436
	AM	0.9151	0.7621	0.6716
Species 3	Mode I	0.8939	0.7414	0.4987
(S3)	Mode II	0.8379	0.7500	0.1985
	AM	**0.9979**	**0.9988**	**0.9761**
Number of sensors (n)		1764	546	779

Numbers in bold mean that these values are the most relevant and were used to make decisions.
[a] The cut-off value for the similarity test at this stage was arbitrarily set at $r = 0.950$.

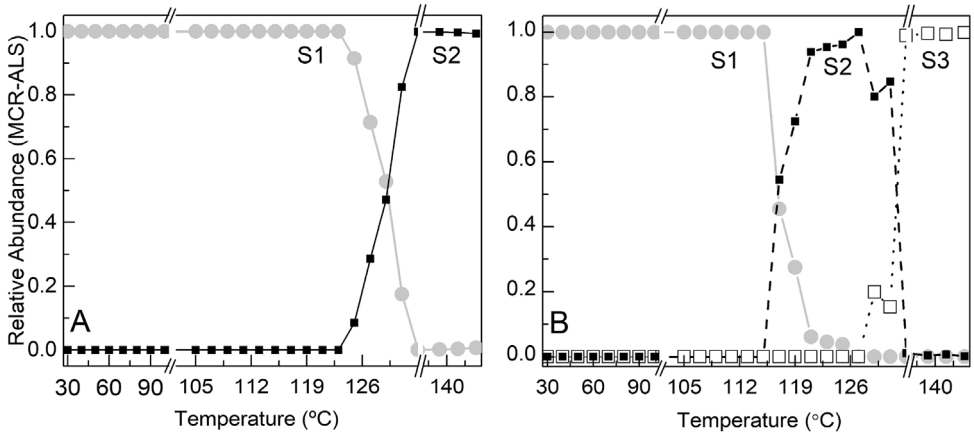

Fig. 6. Temperature-dependent evolution of the different species during the thermal heating process as estimated by MCR-ALS. A) The two species S1 (●) and S2 (■) found in NIM Mode I analysis and B) those found for NIM Mode II S1 (●) S2 (■) and S3 (□).

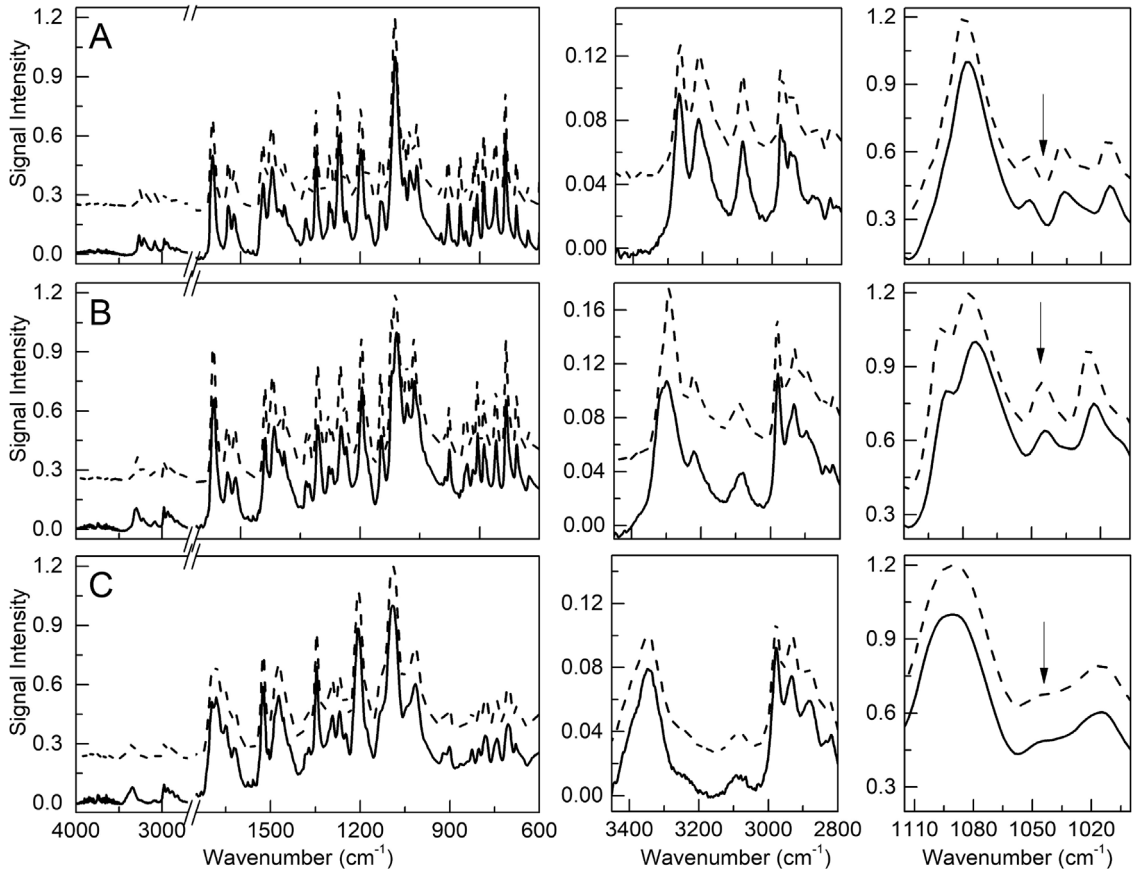

Fig. 7. Comparison between MCR-ALS spectra (– –) and reference spectra (—) involved in the transformation of Mode II for A) S1 vs Mode II; B) S2 vs Mode I; and C) S3 vs AM, respectively. The middle and right column of graphics are expansions in the 3450–2850 cm^{-1} and 1110–1000 cm^{-1} regions, respectively. The arrows point to a characteristic peak for Mode I (1044 cm^{-1}).

which is related to its melting event, consistent with the value shown in Table 1.

When the effect of heating the solid Mode II was monitored, the application of PCA to the ATR-FTIR data matrix revealed the presence of three relevant spectral components (Table 3). Therefore, the MCR-ALS calculation was initialized with three components, including the spectra of the solid forms Mode I, Mode II, and AM, using the set of restrictions mentioned above. The species distribution is shown in Fig. 6B and the variance explained by MCR-ALS for this system was 98.74%.

The pair-wise statistical comparison between the spectra of the "pure" forms S1-S3 and the reference spectra of the different solids (Mode I, Mode II and the AM species) of NIM gave the results presented in Table 5. As expected, S1 was well-correlated with Mode II, exhibiting Pearson's coefficient values of 0.9936, 0.9917 and 0.9776 for the full spectrum, the fingerprint area and the region from 3600 to 2500 cm^{-1}, respectively.

Comparison of S2 with the set of reference spectra at the full spectrum level furnished *r* values of 0.9832, 0.8844 and 0.9151 for Mode I, Mode II and the AM species, respectively, thus, S2 was

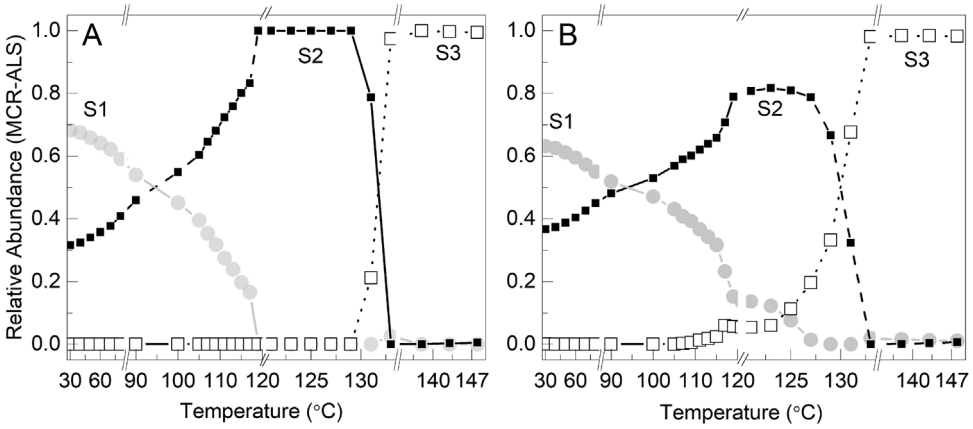

Fig. 8. A) Concentration profiles obtained by ATR-FTIR/MCR-ALS monitoring of the heat-mediated transformation of a commercial sample of NIM. B) Concentration profiles obtained by ATR-FTIR/MCR-ALS monitoring of the heat-mediated transformation of a synthetic sample containing Mode I and Mode II of NIM.

Table 6
Summary of the observed transformations and their corresponding lack of fit parameters.

Sample	Transition temperature (°C)	Transition	Explained variance (%)	Lack of fit (%)	
				PCA	Explained
Mode I	129.2	Mode I → Molten solid	99.75	0.85	5.01
Mode II	116.8 131.9	Mode II → Mode I Mode I → Molten solid	98.74	10.21	11.21
NIM bulk drug Commercial	95.0 131.6	Mode II → Mode I Mode I → Molten solid	99.80	3.86	4.46
Mixture of Mode I and Mode II	94.3 130.0	Mode II → Mode I Mode I → Molten solid	99.90	3.63	4.86

identified as Mode I. Finally, S3 was assigned to the AM species, which displayed correlation coefficients greater than 0.95 in the three spectral regions studied. A comparison between the "pure" spectra furnished by the MCR-ALS algorithm at the full spectrum level for the treatment of Mode II is shown in Fig. 7.

Therefore, the spectral information recovered from the MCR-ALS deconvolution of the heat-mediated transformation of Mode II revealed at least three distinct forms, including both microcrystalline solids, Mode II and Mode I, and the glassy AM solid.

The transition temperature between both crystalline forms extracted from the concentration profile (Fig. 6B) was in full agreement with the temperature reported in the literature for Mode II (116.8 °C). The transition temperature from Mode I to the AM solid was 131.9 °C, also in full agreement with the literature.

The availability of redundant ways for the determination of properties of the solid state of active pharmaceutical ingredients is always welcome. Hence, confirmation of literature results [7] through the developed ATR-FTIR/MCR-ALS method provides a suitable alternative to assess the critical parameters employed for process monitoring or quality control purposes.

3.3. Application to commercial samples

In order to further test the potential of the method a more complex, real system, was examined. Hence, once the transitions of the NIM polymorphs were determined, a commercial sample of NIM was analyzed following the same heating procedure, as well as, data acquisition and treatment. When the PCA analysis was performed, three components were determined as responsible for the 98.83% of spectroscopic signal changes. Then, their MCR-ALS resolution was carried out, obtaining a PCA-lack of fit value of 3.86%. The concentration profiles and "pure" spectra of the species resulting from the MCR-ALS analysis enabled their assignment to the different forms of NIM. The analysis of the concentration curves along the heating profile revealed the presence of two transitions (Fig. 8A), reminiscing the behavior of Mode II. This was not expected, since the most common commercial form of NIM should be Mode I.

However, in an a more in-depth analysis, a decrease in both transition temperatures was noted, being 95 °C for the Mode II→Mode I interconversion and 131.6 °C for the melting event. It was conjectured that, probably this behavior was the result of the presence of mixtures of Mode I and Mode II in the commercial sample (solid). This conjecture agreed with the initial relative abundances of both modifications according to their concertation profiles (Fig. 8A), which should be 68% of Mode II and 32% of Mode I.

Further, when the DSC thermogram of the commercial sample was examined, three endothermic peaks were observed (Fig. 3B). This was interpreted as the result of the presence of an important quantity of Mode II. In this scenario, the fusion of Mode II would take place at 114.5 °C (endothermic peak), followed by recrystallization evidenced by the subsequent exothermic event of small magnitude.

Then, the second endothermic peak at 122.5 °C should represent the melting of the eutectic mixture, where Mode I is the major form and, finally, the third endothermic peak 124.8 °C can be associated to the melting event of Mode I. These conjectures are in agreement with the literature for a mixture of both modifications, confirming that the supplementary peak at 122.5 °C is not caused by an impurity nor an additional modification [7].

In order to further verify this hypothesis, a synthetic sample containing a mixture of Mode I and Mode II was prepared by weighing and mixing the pure polymorphs and analyzed under the standardized conditions. Again, the PCA analysis suggested the presence of three main components and their resolution by MCR-ALS was performed with a PCA-lack of fit value of 3.63%.

Not surprisingly, a behavior analogous to that of the commercial sample was observed (Fig. 8B). This system exhibited a transition

temperature of 94.3 °C for the Mode II → Mode I transformation and the melting temperature of Mode I was 130.0 °C A short summary of the characteristic temperatures of the various transitions found during the analysis of the different samples is presented in Table 6, along with the corresponding lack of fit parameters.

Previously, pure polymorphs of NIM were examined by XRPD and CP-MAS NMR, and polymorphic mixtures of the drug have been examined by DSC for qualitative purposes [7], because of its inability to provide accurate quantitative results on these mixtures. On the contrary, the ATR-FTIR/MCR-ALS approach could provide an alternate means to quantitate the amount of each polymorph of NIM in commercial samples.

4. Conclusions

An ATR-FTR/MCR-ALS method was successfully developed and employed to perform a detailed analysis of the behavior of both crystalline forms of NIM (Mode I and Mode II) in the presence of a thermal stress condition, and to study the phase transitions. Monitoring the whole processes was simply and efficiently achieved in relatively short time and with minimum sample manipulation.

To that end, both polymorphic forms of NIM were prepared and fully characterized employing thermal (DSC, melting point), spectroscopic (FTIR, Raman), diffractometric (X-ray of the powder) and microscopic (SEM) analytical techniques.

Mode I presented a single transition related to its melting event at 129.2 °C, while Mode II exhibited two transitions. The first one at 116.8 °C, related to the melting point of Mode II and its further transformation into Mode I, and the second at 131.9 °C related to the transition from Mode I to its molten phase, which further gives an amorphous solid form upon cooling.

Knowledge of basic properties of polymorphic drug substances enables the adjustment of processing conditions to anticipate and prevent potential polymorphic transformations. The proposed method was applied to synthetic and commercial polymorphic mixtures of NIM, allowing the identification of the species (Mode II and Mode I), as well as to obtain the estimation of the Mode II:Mode I ratio and the determination of their transition temperatures. Therefore, it should be considered as a suitable strategy with great potential to monitor and observe the behavior of solid forms of active pharmaceutical ingredients as a function of temperature variation, in different scenarios.

Acknowledgments

The authors thank CONICET (PUE IQUIR 2016) and ANPCyT (PICT 2014-0445) for financial support. Thanks are also due to the ASACTeI (Institutional grant AC 2015-00005 for a 400 MHz NMR machine). N.L.C. is thankful to CONICET for her Doctoral Fellowship and also to AUGM for a travel scholarship (Escala Program, 2015).

References

[1] H.G. Brittain, Polymorphism in Pharmaceutical Solids, 2nd ed., Informa Healthcare, Inc., New York, USA, 2009.
[2] J. Sood, B. Sapra, S. Bhandari, M. Jindal, A.K. Tiwary, Understanding pharmaceutical polymorphic transformations I: influence of process variables and storage conditions, Ther. Deliv. 5 (2014) 1123–1142.
[3] L. Zhang, Z. Song, Y. Dong, Y. Wang, X. Li, H. Long, K. Xu, C. Deng, M. Meng, Y. Yin, R. Xi, Enantiomeric separation of 1,4-dihydropyridines by liquid-phase microextraction with supercritical fluid chromatography, J. Supercrit. Fluids 107 (2016) 129–136.
[4] H. Nguyen, Bioequivalence reviews: ANDA 76, in: Division of Bioequivalence Review, U.S Food and Drug Administration, 2004.
[5] S.C. Sweetman, Nimodipine, in: S.C. Sweetman (Ed.), Martindale: The Complete Drug Reference, Pharmaceutical Press, London, UK, 2009, pp. 1357–1358.
[6] Z. Guo, M. Ma, T. Wang, D. Chang, T. Jiang, S. Wang, A kinetic study of the polymorphic transformation of nimodipine and indomethacin during high shear granulation, AAPS PharmSciTech 12 (2011) 610–619.
[7] A. Grunenberg, B. Keil, J.-O. Henck, Polymorphism in binary mixtures, as exemplified by nimodipine, Int. J. Pharm. 118 (1995) 11–21.
[8] G.Z. Papageorgiou, D. Bikiaris, E. Karavas, S. Politis, A. Docoslis, Y. Park, A. Stergiou, E. Georgarakis, Effect of physical state and particle size distribution on dissolution enhancement of nimodipine/PEG solid dispersions prepared by melt mixing and solvent evaporation, AAPS J. 8 (2006) 623–631.
[9] H.-J. Yuan, D.-W. Chen, L.-J. Fan, Y. Ren, Study on influencing factors of chemical stability of nimodipine polymorphs, Chin. Pharm. J. 40 (2005) 1871–1873.
[10] T. Mazon Cardoso, P. Oening Rodrigues, H.K. Stulzer, M.A. Segatto Silva, Physical-chemical characterization and polymorphism determination of two nimodipine samples deriving from distinct laboratories, Drug Dev. Ind. Pharm. 31 (2005) 631–637.
[11] X.D. Liu, L. Xie, G.Q. Xu, J. Wang, Y.C. Zhou, G.Q. Liu, Variability of nimodipine pharmacokinetics in healthy Chinese males, Chin. J. Pharmacol. Toxicol. 10 (1996) 25–27.
[12] A. Siddiqui, Z. Rahman, V.A. Sayeed, M.A. Khan, Chemometric evaluation of near infrared, Fourier transform infrared, and Raman spectroscopic models for the prediction of nimodipine polymorphs, J. Pharm. Sci. 102 (2013) 4024–4035.
[13] Nimodipine Capsule Recall, Food and Drug Administration, Sun Pharmaceutical Industries, Inc. issues nationwide voluntary recall of one lot of nimodipine capsules due to crystallization of the fill material, Rockville, MD, USA, 2013 (Accessed 20 January 2018) https://www.fdanews.com/articles/149289-sun-recalls-nimodipine-capsules-on-crystallization-concerns.
[14] X. Yang, W. Ke, P. Zi, F. Liu, L. Yu, Detecting and identifying the complexation of nimodipine with hydroxypropyl-β-cyclodextrin present in tablets by Raman spectroscopy, J. Pharm. Sci. 97 (2008) 2702–2719.
[15] Y. Zu, N. Li, X. Zhao, Y. Li, Y. Ge, W. Wang, K. Wang, Y. Liu, In vitro dissolution enhancement of micronized l-nimodipine by antisolvent re-crystallization from its crystal form H, Int. J. Pharm. 464 (2014) 1–9.
[16] N.A. Urbanetz, B.H. Lippold, Solid dispersions of nimodipine and polyethylene glycol 2000: dissolution properties and physico-chemical characterization, Eur. J. Pharm. Biopharm. 59 (2005) 107–118.
[17] A. Gorajana, N. Koteswara, W. Rao, Yuen Nee, Physicochemical characterization and in vitro evaluation of solid dispersions of nimodipine with PEG 8000, Asian J. Chem. 23 (2011) 2857–2859.
[18] G.Z. Papageorgiou, A. Docoslis, M. Georgarakis, D. Bikiaris, The effect of physical state on the drug dissolution rate miscibility studies of nimodipine with PVP, J. Therm. Anal. Calorim. 95 (2009) 903–915.
[19] M. Klüppel Riekes, T. Caon, J. da Silva Jr, R. Sordi, G. Kuminek, L. Sakis Bernardi, C.R. Rambo, C.E. Maduro de Campos, D. Fernandes, H.K. Stulzer, Enhanced hypotensive effect of nimodipine solid dispersions produced by supercritical CO_2 drying, Powder Technol. 278 (2015) 204–210.
[20] J. Li, Q. Fu, X. Liu, M. Li, Y. Wang, Formulation of nimodipine nanocrystals for oral administration, Arch. Pharm. Res. 39 (2016) 202–212.
[21] Z. He, D. Zhong, X. Chen, X. Liu, X. Tang, L. Zhao, Development of a dissolution medium for nimodipine tablets based on bioavailability evaluation, Eur. J. Pharm. Sci. 21 (2004) 487–491.
[22] M.K. Riekes, G. Kuminek, G.S. Rauber, S.L. Cuffini, H.K. Stulzer, Development and validation of an intrinsic dissolution method for nimodipine polymorphs, Cent. Eur. J. Chem. 12 (2014) 549–556.
[23] Q. Fu, L. Kou, C. Gong, M. Li, J. Sun, D. Zhang, M. Liu, X. Sui, K. Liu, S. Wang, Z. He, Relationship between dissolution and bioavailability for nimodipine colloidal dispersions: the critical size in improving bioavailability, Int. J. Pharm. 427 (2012) 358–364.
[24] A. Docoslis, K.L. Huszarik, G.Z. Papageorgiou, D. Bikiaris, A. Stergiou, E. Georgarakis, Characterization of the distribution, polymorphism, and stability of nimodipine in its solid dispersions in polyethylene glycol by micro-Raman spectroscopy and powder X-ray diffraction, AAPS J. 9 (2007) 361–370.
[25] M.K. Riekes, R.N. Pereira, G.S. Rauber, S.L. Cuffini, C.E.M. de Campos, M.A.S. Silva, H.K. Stulzer, Polymorphism in nimodipine raw materials: development and validation of a quantitative method through differential scanning calorimetry, J. Pharm. Biomed. Anal. 70 (2012) 188–193.
[26] A. Siddiqui, Z. Rahman, M.A. Khan, Application of chemometric methods to differential scanning calorimeter (DSC) to estimate nimodipine polymorphs from cosolvent system, Drug Dev. Ind. Pharm. 41 (2015) 995–999.
[27] Z. Rahman, A. Mohammad, A. Siddiqui, M.A. Khan, Comparison of univariate and multivariate models of ^{13}C ssNMR and XRPD techniques for quantification of nimodipine polymorphs, AAPS PharmSciTech 16 (2015) 1368–1375.
[28] N.L. Calvo, R.M. Maggio, T.S. Kaufman, Characterization of pharmaceutically relevant materials at the solid state employing chemometrics methods, J. Pharm. Biomed. Anal. 147 (2018) 538–564.
[29] N.L. Calvo, R.M. Maggio, T.S. Kaufman, Chemometrics-assisted solid-state characterization of pharmaceutically relevant materials. Polymorphic substances, J. Pharm. Biomed. Anal. 147 (2018) 518–537.
[30] J. Priotti, A.V. Codina, D. Leonardi, M.D. Vasconi, L.I. Hinrichsen, M.C. Lamas, Albendazole microcrystal formulations based on chitosan and cellulose derivatives: physicochemical characterization and in vitro parasiticidal activity in Trichinella spiralis adult worms, AAPS PharmSciTech 18 (2017) 947–956.
[31] P. Barmpalexis, K. Kachrimanis, E. Georgarakis, Solid dispersions in the development of a nimodipine floating tablet formulation and optimization by

artificial neural networks and genetic programming, Eur. J. Pharm. Biopharm. 77 (2011) 122–131.
[32] K. Drużbicki, A. Pajzderska, A. Kiwilsza, J. Jenczyk, D. Chudoba, M. Jarek, J. Mielcarek, J. Wąsicki, In search of the mutual relationship between the structure, solid-state spectroscopy and molecular dynamics in selected calcium channel blockers, Eur. J. Pharm. Sci. 85 (2016) 68–83.
[33] G.M. Mohan Babu, N. Kumar, K. Sankar, B. Ram, N. Kumar, K. Murthy, In vivo evaluation of modified gum karaya as a carrier for improving the oral bioavailability of a poorly water-soluble drug, nimodipine, AAPS PharmSciTech 3 (2002) 55–63.
[34] Y. Hu, X. Jiang, Y. Ding, L. Zhang, C. Yang, J. Zhang, J. Chen, Y. Yang, Preparation and drug release behaviors of nimodipine-loaded poly(caprolactone)-poly(ethylene oxide)-polylactide amphiphilic copolymer nanoparticles, Biomaterials 24 (2003) 2395–2404.
[35] X. Tang, M. Pikal, L. Taylor, A spectroscopic investigation of hydrogen bond patterns in crystalline and amorphous phases in dihydropyridine calcium channel blockers, Pharm. Res. 19 (2002) 477–483.
[36] X. Zheng, R. Yang, X. Tang, L. Zheng, Part I: characterization of solid dispersions of nimodipine prepared by hot-melt extrusion, Drug Dev. Ind. Pharm. 33 (2013) 791–802.
[37] S. Papadimitriou, G.Z. Papageorgiou, F.I. Kanaze, M. Georgarakis, D.N. Bikiaris, Nanoencapsulation of nimodipine in novel biocompatible poly(propylene-co-butylene succinate) aliphatic copolyesters for sustained release, J. Nanomater. (2009), 716242, http://dx.doi.org/10.1155/2009/716242, 11 pages.
[38] J. Jaumot, R. Gargallo, A. de Juan, R. Tauler, A graphical user-friendly interface for MCR-ALS: a new tool for multivariate curve resolution in MATLAB, Chemom. Intell. Lab. Syst. 76 (2005) 101–110.